Extracting the spectral signature of alpha-clustering in 44,48,52Ti using the continuous wavelet transform

BAILEY, Sam, KOKALOVA, Tzany, FREER, Martin, WHELDON, Carl, SMITH, Robin <http://orcid.org/0000-0002-9671-8599>, WALSHE, Joseph, CURTIS, Neil, SOIC, Neven, PREPOLEC, Lovro, TOKIC, Vedrana, MIGUEL MARQUES, Francisco, ACHOURI, Lynda, DELAUNAY, Franck, DESHAYES, Quentin, PARLOG, Marian, FERNANDEZ-DOMINGUEZ, Beatriz, JAQUOT, Bertrand and SOYLU, Asim

Extracting the spectral signature of α-clustering in ^{44,48,52}Ti using the continuous wavelet transform

Sam Bailey,[1] Tzany Kokalova,[1,*] Martin Freer,[1] Carl Wheldon,[1] Robin Smith,[1,†] Joseph Walshe,[1] Neil Curtis,[1] Neven Soić,[2] Lovro Prepolec,[2] Vedrana Tokić,[2] Francisco Miguel Marqués,[3] Lynda Achouri,[3] Franck Delaunay,[3] Quentin Deshayes,[3] Marian Parlog,[3,4] Beatriz Fernández-Dominguez,[5] and Bertrand Jacquot[6]

[1] *School of Physics and Astronomy, University of Birmingham, Birmingham, B15 2TT, UK.*
[2] *Institut Ruđer Bošković, Bijenička cesta 54, 10000 Zagreb, Croatia.*
[3] *Laboratoire de Physique Corpusculaire de Caen, 6 bd Maréchal Juin, 14050 Caen Cedex, France.*
[4] *'Horia Hulubei' National Institute of Physics and Nuclear Engineering (IFIN-HH), RO-077125 Bucharest Magurele, Romania.*
[5] *Universidade de Santiago de Compostela, Praza do Obradoiro, 15782 Santiago de Compostela, Spain.*
[6] *Grand Accélérateur National d'Ions Lourds, Bd Henri Becquerel, BP 55027 - 14076 Caen Cedex 05, France.*

(Dated: September 12, 2019)

A novel technique has been developed, making use of the continuous wavelet transform to identify α-clustered states from resonant scattering measurements in regions of high nuclear state density. This technique expedites the investigation of α-clustering in medium mass and heavy nuclei, where the role that α-clustering plays in the structure of the nucleus is poorly understood. Here we report the application of this technique to measurements of the ^{4}He(^{40,44,48}Ca,α) resonant reactions, leading to an assessment of the α-cluster structure of ^{44,48,52}Ti. Alpha-clustering was identified in ^{44}Ti and ^{52}Ti, but was observed to break down in ^{48}Ti. The implications of these results are discussed.

PACS numbers: 21.60.Gx, 25.60.Bx, 27.40.+z, 29.85.Fj

The atomic nucleus is a complex many-body quantum system which, 105 years after its discovery by Rutherford [1], is still not fully understood. Historically there have been a plethora of different attempts to explain the structure of the nucleus, the most famous of which is the nuclear shell model. This model is built upon the mean-field assumption that the interactions between all of the nucleons in the nucleus average out, allowing each nucleon to be treated independently, moving in a 'mean-field' potential which reflects this average interaction. The considerable success of this model, especially for heavy nuclei, is generally interpreted as vindication of this underlying assumption, implying that nuclei do, in most cases, behave similarly to a collection of independent protons and neutrons moving in a mean-field potential.

The mean-field description of the nucleus is not, however, universally applicable, and the shell model fails to provide a reasonable description of some of the more exotic features of nuclear structure. An example of a phenomenon that the shell model fails to predict is the condensation of nucleons into sub-structures within the nucleus, known as clusters. This behaviour is known as nuclear clustering, and the most common type is α-clustering, where at least one of the clusters formed in the nucleus is the α-particle.

The formation of α-clusters has been shown to be crucial when describing the structural properties of many light nuclei [2, 3], however, it is equally apparent that the mean-field picture of the nucleus describes the properties of heavy nuclei very well, suggesting that coherent phenomena such as clusters in most cases do not contribute significantly to their structure. In the pursuit of a clear and consistent understanding of nuclear structure, it is therefore of significant interest to explore why certain nuclei seem to exhibit clear alpha clustering (alongside mean-field structures), while other nuclei do not. The pursuit of this question has led to considerable experimental and theoretical work investigating α-clustering in medium mass nuclei [4], in an attempt to ascertain the degree to which clustering survives with increasing nuclear mass.

Titanium-44 has been the focus of many studies of α-clustering in the medium mass regime, with the experimental identification of α-clustered structures using both α-transfer reactions [5–7] and resonant α scattering [8, 9]. Much of this experimental work was summarised, and shown to be in good agreement with α-cluster model calculations in reference [4, ch. 2]. More recently, a deformed basis Antisymmetrised Molecular Dynamics (AMD) calculation has shown ^{44}Ti to be composed of *both* α-clustered and mean-field type structures [10]. This rich variety of structures suggests that Ti isotopes may provide an excellent opportunity to examine how the interplay between clustered and mean-field type structures develops in medium mass nuclei.

A difficulty faced by experimental projects in this field is in the analysis of the complex spectra resulting from the high level density associated with heavier systems. This article reports a new technique for analysing such nuclei, and the results of its application to a recently performed measurement of the ^{4}He(^{40,44,48}Ca,α) reactions and the assessment of α-clustering in ^{44,48,52}Ti. This

* Corresponding author: t.kokalova@bham.ac.uk
† Present address: Department of Engineering and Mathematics, Sheffield Hallam University, City Campus, Howard Street, Sheffield, S1 1WB, UK

technique combines the Thick Target Inverse Kinematics (TTIK) approach to making resonant scattering measurements [11] with the Continuous Wavelet Transform (CWT) [12] in the analysis of those measurements. The CWT was developed for use in signal processing and image analysis, but has been used more recently in nuclear structure physics to extract the fine structure of giant resonances [13, 14] and in the analysis of inelastic α-particle scattering on ^{16}O [15].

TTIK measurements use a heavy beam incident on a thick gas target. A window is used to separate the gas target from the evacuated beam line. The beam mainly interacts with the electrons in the gas target, which causes it to lose energy as it traverses the gas [16]. The beam also interacts with the target via nucleus-nucleus collisions, and the light decay products of these nuclear reactions are recorded using detectors placed inside the reaction chamber. These measurements, combined with the energy loss of the beam through the target, lead to a continuous measurement of the entire excitation spectrum from a single initial beam energy. It is common practice to place the detectors at 0° to the beamline and at the opposite end of the chamber to the beam entrance, allowing measurements to be made at a scattering angle of 180° in the centre-of-mass frame. This is preferable since 180° corresponds to the minimum for the Rutherford contribution to the cross-section and the maximum for the resonant contribution, producing the clearest possible resonant spectra. The beam energy and gas pressure are tuned to ensure that the beam is stopped in the gas before it reaches the detectors.

The TTIK technique is an especially effective tool for the investigation of α-clustering since it is very easy to set up with a ^{4}He gas target, which populates states in the compound nucleus through the α-channel and as such preferentially populates α-clustered states. These states manifest themselves in the excitation spectra as resonances, and it is from the analysis of these resonances that structural information can be extracted. This analysis usually relies on R-matrix theory [17], which is used either in its full form or a simplified form [18] to fit the experimental data and extract the properties of the compound nuclear states. However, this process is often found to be especially challenging when applied to TTIK measurements of nuclei with a high level density, because of the deterioration of the energy resolution for scattering angles away from 180° [19, 20]. Our new technique is unique since it does not require angular distribution measurements, thus giving the opportunity to perform only a single measurement at 180°, ensuring optimal resolution.

It has been observed in a series of TTIK measurements investigating α-clustering in ^{32}S, ^{34}S, ^{36}Ar and ^{40}Ca, that α-clustered states in medium mass nuclei are often fragmented into many states with the same spin and parity, J^π, by the coupling of clustered states to non-clustered states [21]. These fragmented states are strongly populated through the α-channel, due to their partially α-clustered structure, and are localised in close proximity to the original α-clustered states.

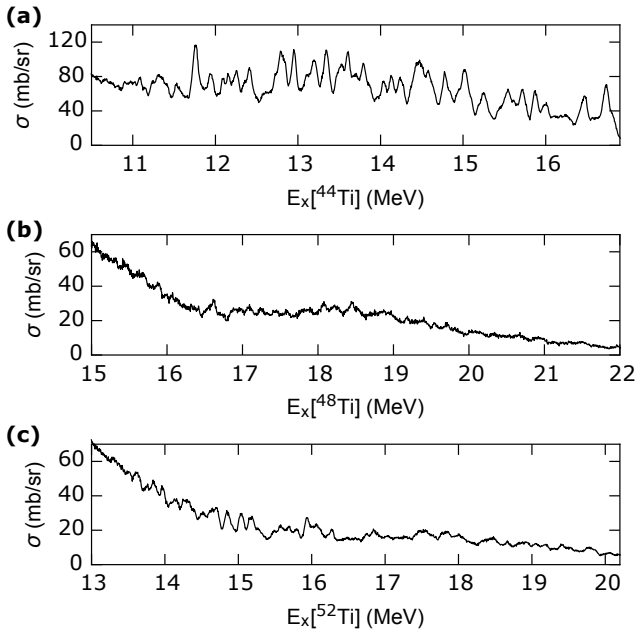

FIG. 1. **Measured excitation spectra. a-c**, Measurements of the differential cross-section, made at a centre of mass scattering angle of 180°, of the ^{4}He(^{40}Ca,α) **(a)**, ^{4}He(^{44}Ca,α) **(b)** and ^{4}He(^{48}Ca,α) **(c)** reactions. The resonances in these measurements are relevant to the structure of ^{44}Ti, ^{48}Ti and ^{52}Ti respectively.

In TTIK measurements these fragmented states manifest themselves as a group of large resonances in the vicinity of the original α-clustered state. Our method uses the CWT to identify these groups of fragmented α-clustered states directly in the experimental spectra, without having to extract the individual energy levels via a time consuming R-matrix fit.

We report here on the application of this new technique to the investigation of α-clustering in ^{44,48,52}Ti using the ^{4}He(^{40,44,48}Ca,α) reactions. The measurements were made at the GANIL radioactive beam facility in Caen, France, using ^{40,44,48}Ca beams at 180, 207 and 234 MeV, respectively. Two 1 mm thick double-sided silicon strip detectors were placed 448 mm from the window separating the reaction chamber and the beamline, and at 0° to the beamline. The scattered α-particles were measured using stacked detectors, and distinguished from other decay products by means of their differential energy loss. The excitation energy of the compound Ti nucleus and position of the reaction in the chamber were calculated, for each event, from the measured energy of the α-particle, by simulating the reaction kinematics, and the energy loss of the beam and α-particles through the ^{4}He gas. For more details on this procedure please refer to [22, Sec. II]. The reconstructed ^{4}He(^{40,44,48}Ca,α) spectra are shown in figure 1. The excitation energy resolution was calculated to be 45 keV at full width half maximum using the Monte-Carlo software REX [19].

The CWT provides a decomposition of the spectra into

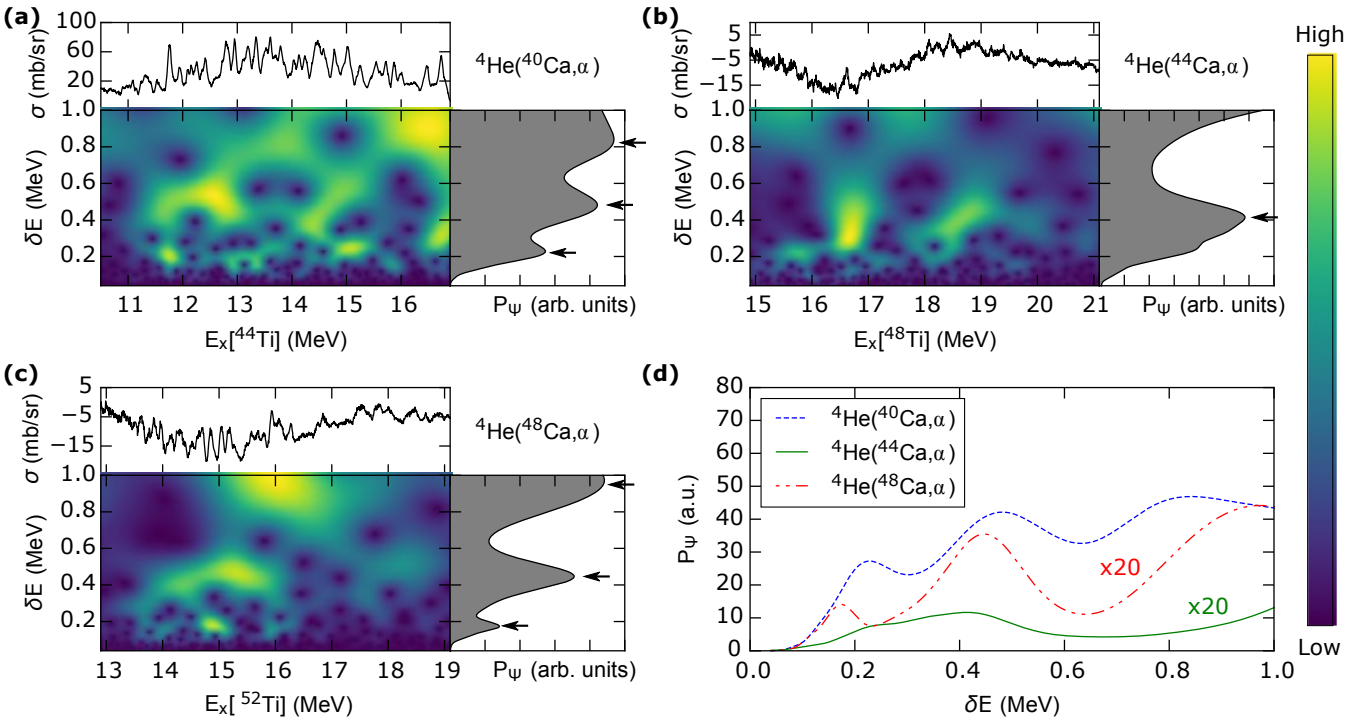

FIG. 2. **The CWT's of the measured spectra. a-c**, Spectrograms of the ^{4}He(^{40}Ca,α) **(a)**, ^{4}He(^{44}Ca,α) **(b)** and ^{4}He(^{40}Ca,α) **(c)** excitation spectra. In each case: measured excitation energy spectrum with the Rutherford contribution subtracted (horizontal spectrum), absolute value of wavelet transform $|W_\Psi|$ (lower coloured 2D plot) and the wavelet power spectrum P_Ψ in arbitrary units (vertical right spectrum). The arrows indicate characteristic energy scales. **(d)**, A comparison of the power spectra for each measurement.

a continuous range of scales δE. The wavelet transform, $W_\Psi(E, \delta E)$, of a spectrum, $\sigma(E)$, represents the contribution of a given scale to the spectrum at a specific energy, E, and is defined as

$$W_\Psi(E, \delta E) = \frac{1}{\sqrt{\delta E}} \int_{-\infty}^{\infty} \sigma(\epsilon) \Psi \left(\frac{\epsilon - E}{\delta E} \right) d\epsilon, \quad (1)$$

where ϵ is a dummy variable used to facilitate the integration and $\Psi(E)$ is an appropriately chosen wavelet. The wavelet power spectrum $P_\Psi(\delta E)$ represents the contribution of a given scale to the entire spectrum and is calculated by integrating $|W_\Psi(E, \delta E)|^2$ over all E,

$$P_\Psi(\delta E) = \int_{-\infty}^{\infty} |W_\Psi(E, \delta E)|^2 \, dE \, . \quad (2)$$

In the following analysis the complex Morlet wavelet is used to characterise the periodic features in the spectrum [12, p. 229], defined as

$$\Psi(E) = \left(d\sqrt{\pi}\right)^{1/2} \exp\left(-i2\pi E\right) \exp\left(-\frac{E}{2d^2}\right), \quad (3)$$

where d dictates the size of the Gaussian envelope, and in this work was chosen empirically to be 0.8. The CWT is often visualised using a spectrogram, which shows $\sigma(E)$, $W_\Psi(E, \delta E)$ and $P_\Psi(\delta E)$ in a single plot.

The spectrograms produced by the application of the CWT to the experimental spectra are displayed in figure 2, in each case the Rutherford contribution is subtracted from the spectra prior to the transformation. All three power spectra present characteristic scales at $\delta E \approx 0.45$ and $\delta E \approx 0.8 - 1.5$ (this is off the scale for ^{48}Ti in figure 2), however, ^{44}Ti and ^{52}Ti both exhibit an additional characteristic scale at $\delta E \approx 0.2$. It is this additional characteristic scale which according to our new technique is indicative of the presence of fragmented α-clustered states in the spectrum.

This additional characteristic scale arises because a set of fragmented α-clustered states all have a partially α-clustered structure, similar to that of the original α-clustered state from which they originated. This means that they would all be expected to have large α partial widths, and small widths for all other open decay channels, leading to consistently strong amplitudes for the fragmented resonances. Additionally, since the fragmented states all have the same J^π, one would expect their spacings to be more regular, following a Wigner distribution [23], than they would be if they had different values of J^π. This combination of regularly spaced states all with similar amplitudes produces a strong periodic structure, which is picked out by the CWT, producing the signature characteristic scale observed in ^{44}Ti and ^{52}Ti. Furthermore, this signature peak is likely to

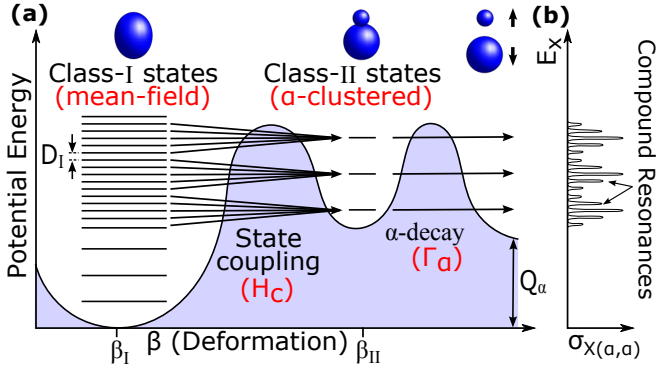

FIG. 3. **A schematic illustration of a double humped fission barrier. (a)**, The application of a double humped fission barrier to fragmented α-clustered states, with class-I and class-II states indicated. Adapted from [25, p. 97–98]. **(b)**, A schematic X(α, α) cross-section resulting from this structure. For simplicity the Rutherford contribution is not shown.

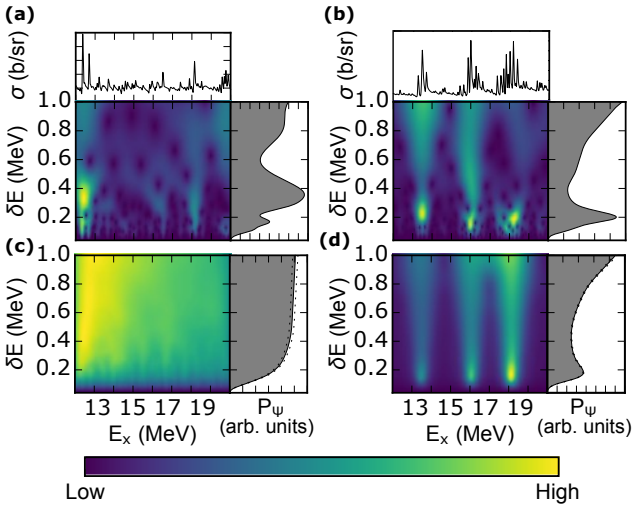

FIG. 4. **A comparison of the CWT's of the simulated spectra with and without coupling to class-II states. (a),(b)**, Spectrogram of a single iteration without coupling to class-II states (**a**) and with coupling to class-II states **(b)**. **(c),(d)**, An average over 500 spectrograms without coupling to class-II states **(c)** and with coupling to class-II states **(d)**. In all cases the class-II states were fixed at $E^{(II)} = 13.5$, 16 and 18 MeV and $\gamma_\alpha^{(II)\,2} = 0.1$ MeV. The set of class-I states was defined by $\langle D_{J^\pi}^{(I)} \rangle = 0.15$ MeV, $\langle \gamma_\alpha^{(I)\,2} \rangle = 0.0005$ MeV and $\langle \gamma_{\mu\neq\alpha}^{(I)\,2} \rangle = 0.01$ MeV. The coupling constant $H_c = 0.1$ MeV.

be the lowest peak in P_Ψ since the fragmented states are expected to be, on average, more densely packed than the rest of the spectrum [24, p. 772].

The emergence of an additional characteristic scale was demonstrated by generating simulated excitation spectra which contain fragmented α-clustered states, and comparing them with the equivalent simulations without the fragmented α-clustered states using the CWT. The fragmented α-clustered spectra were generated by coupling a set of highly deformed α-clustered states (class-II states) to a set of mean-field type states (class-I states), using the techniques developed for the treatment of double humped fission barriers by Bjørnholm and Lynn [24]. This procedure produced a set of compound states, from which an excitation spectrum could be calculated. A pictorial representation of this process is displayed in figure 3. The spectra without fragmented α-clustered states were calculated using the uncoupled set of class-I states.

The class-I states were required to be as generally representative of a generic mean-field type nucleus as possible. This was done by randomising the excitation energies, $E^{(I)}$, reduced widths, $\gamma_\mu^{(I)}$ and spins and parities, J^π, such that they adhered to the appropriate statistical distributions [26, Sec. I. B]. Here μ denotes each open decay channel. The nearest neighbour state spacing between states of the same J^π, $D_{J^\pi}^{(I)}$, was assumed to follow a Wigner distribution [23],

$$P(D_{J^\pi}^{(I)})dD_{J^\pi}^{(I)} = \frac{\pi D_{J^\pi}^{(I)}}{2\langle D_{J^\pi}^{(I)}\rangle^2} \exp\left(-\frac{\pi D_{J^\pi}^{(I)\,2}}{4\langle D_{J^\pi}^{(I)}\rangle^2}\right) dD_{J^\pi}^{(I)}, \quad (4)$$

where $\langle D_{J^\pi}^{(I)} \rangle$ defines the mean state spacing. The reduced widths were assumed to follow a normal distribution with variance $\langle \gamma_\mu^2 \rangle$ [27, Sec. 11.1.1]. Both of these distributions are well established and have been successful in replicating the experimental distributions of many nuclei [26, Sec. I. B].

The α-clustered class-II states were defined to have large $\gamma_\alpha^{(II)}$, and negligible reduced widths for all other open channels. Their energies, $E^{(II)}$, and J^π were chosen arbitrarily, since the results were found to be independent of these variables. They were coupled only to class-I states of the same J^π, with a constant coupling strength, dictated by the coupling constant, H_c, using the procedure detailed in reference [24, p. 771].

The simulated excitation spectra were calculated from the compound states using the Simplified R-Matrix for spinless particles [21]. The background phase shifts, which dictate the interference between the resonant contributions and background contribution to the excitation spectra, were randomised between 0 and 2π.

The spectra were simulated for a range of different values for H_c, $\langle D_{J^\pi}^{(I)} \rangle$, $\langle \gamma_\alpha^{(I)2} \rangle$, $\langle \gamma_{\mu\neq\alpha}^{(I)2} \rangle$ and $\gamma_\alpha^{(II)}$. The results discussed below were found in all cases where the following conditions were satisfied: the mean state spacing was larger than the average level width to ensure that the resonances were resolvable, H_c was large enough to ensure significant clustered state fragmentation and the α-clustered states had much larger α-widths than the mean-field type states. It has been argued that for nuclei in this mass and energy region that one would expect the resonances to be resolvable, and the contribution due to Ericson fluctuations should be minimal [21].

The CWT's were averaged over many simulations with different sets of class-I states to identify the average response of the CWT to fragmented α-clustered states. A

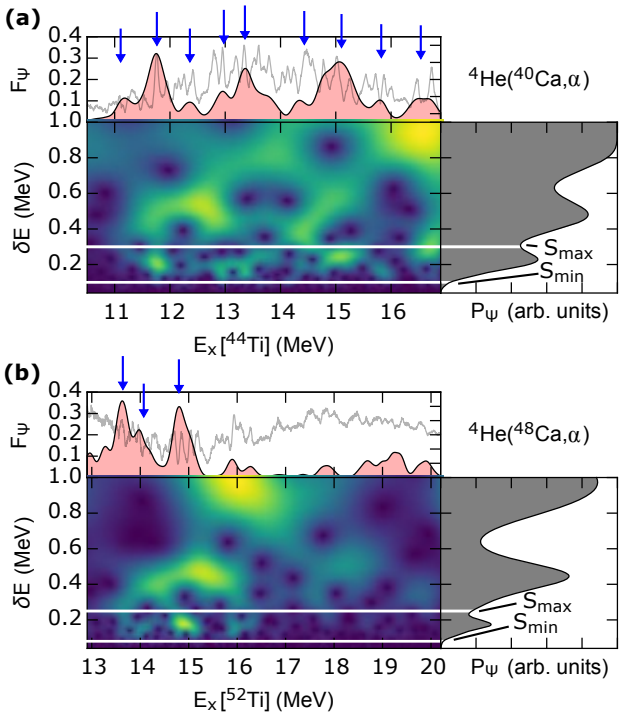

FIG. 5. **CWT's of the measured spectra with an F_Ψ analysis a,b**. Spectrograms as in figure 2 for ^{44}Ti **(a)** and ^{52}Ti **(b)**. The quantity F_Ψ is calculated between S_{min} and S_{max} (white lines), and overlaid in red on the spectra. The blue arrows indicate the α-clustered states extracted from this analysis.

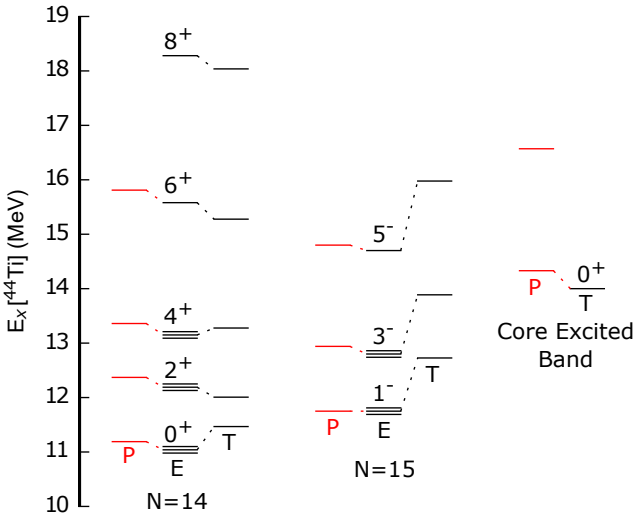

FIG. 6. **A comparison between the previously measured high lying α-clustered states in ^{44}Ti and those extracted in the present work.** The states extracted in the present work are shown in red, denoted by P. Those measured previously are denoted by E, and theoretical energy levels predicted by an α-cluster model are denoted by T. States that have been observed previously as groups of fragmented states are shown as 3 lines. This figure is adapted from Fig. 29 in reference [4, ch. 2], and both the previously measured and theoretically predicted energy levels are taken from that work.

typical example of the results is displayed in figure 4. A significant enhancement was observed in P_Ψ at low δE in the average over the CWT's of the spectra containing α-clustered states, which was generated by an increased likelihood of the existence of a sharp characteristic scale at low δE. This enhancement was not observed in the spectra which did not contain fragmented α-clustered states.

It is also clear from figure 4 that this large characteristic scale is composed of hot-spots in W_Ψ, one for each set of fragmented α-clustered states. These results are consistent with the observation of the additional characteristic scales in ^{44}Ti and ^{52}Ti, which are the lowest clear peaks in P_Ψ, and can be seen to be composed of these trademark hot-spots. By contrast the first characteristic scale in ^{48}Ti is too high and too broad to be considered a signature peak.

The hot-spots in W_Ψ may be used to extract the energies of the α-clustered states. The fraction of W_Ψ that originates from within the boundaries of the signature peak: $[S_{min}, S_{max}]$, should be enhanced by the hot-spots, identifying the α-clustered states as peaks. This quantity, F_Ψ, is defined formally as

$$F_\Psi(E) = \frac{\int_{S_{min}}^{S_{max}} |W_\Psi(E,\delta E)|^2 d\,\delta E}{\int_0^\infty |W_\Psi(E,\delta E)|^2 d\,\delta E}\,. \qquad (5)$$

The results of this calculation are shown in figure 5 for ^{44}Ti and ^{52}Ti, under the assumption that the lowest characteristic scale is the signature peak. Based on this, the following α-clustered states were identified at $E_x \approx$ 11.19, 11.75, 12.37, 12.94, 13.36, 14.33, 14.8, 15.81 and 16.57 MeV in ^{44}Ti and at $E_x \approx$ 13.66, 14.0 and 14.8 MeV in ^{52}Ti. Each of these states must be fragmented in order to be measured using our technique.

A comparison with a summary of the previously identified α-clustered states in ^{44}Ti [4, ch. 2] is shown in figure 6. An excellent one-to-one agreement is observed between the states extracted in this work using the spectral signature analysis, and those measured in previous studies. These results also extend the current understanding of ^{44}Ti, providing the first experimental evidence for the fragmented nature of the 5^- and 6^+ states in the $N = 14$ and $N = 15$ rotational bands, which was expected based on the fragmented nature of the lower spin members of those bands, but had not been observed experimentally. We also observe the first measurement of the predicted 0^+ state in the core excited band, and make a tentative suggestion that the state observed at 16.57 MeV may be the 2^+ state in this band, since it cannot be assigned to any previously known or predicted state. It is important to note that these assignments are made based on the agreement in excitation energies alone, as the spins and parities of the states are not extracted using the spectral

signature technique.

To conclude, the application of the CWT to the analysis of TTIK measurements has been used to extract the spectral signature of fragmented α-clustering in medium mass nuclei, leading to an assessment of the development of α-clustering in neutron rich Ti isotopes. A fragmented α+^{40}Ca structure was confirmed in ^{44}Ti, showing good agreement with previous work. This structure was not observed in ^{48}Ti but re-emerges in ^{52}Ti, with the first measurement of α-clustered states in this nucleus. This suggests that the doubly magic nature of the ^{40}Ca and ^{48}Ca cores may play an important role in generating the cluster structure, but further theoretical development is required in this direction.

ACKNOWLEDGMENTS

The authors would like to thank the STFC (grant number 1200042) and ENSAR for their financial support, and the GANIL facility for the delivery of the beams and the experimental preparation.

[1] E. Rutherford, Philosophical Magazine **21**, 669 (1911).
[2] M. Freer and A.C. Merchant J. Phys. G **23**, 261 (1997).
[3] W. von Oertzen, M. Freer and Y. Kanada-En'yo, Phys. Rep. **432**, 43 (2006).
[4] S. Ohkubo, M. Fujiwara and P.E. Hodgson, *Alpha-clustering and molecular structure of medium-weight and heavy nuclei*, Chapter 1 - Introduction, Progress of Theoretical Physics Supplement **132**, 1 (1999) and T. Sakuda; S. Ohkubo, *Microscopic Study of Coexistence of Alpha-Cluster and Shell-Model Structure in the ^{40}Ca-^{44}Ti Region*, Chapter 4, Progress of Theoretical Physics Supplement **132**, 103 (1999).
[5] T. Yamaya, *et al.*, Phys. Rev. C **42**, 1935 (1990).
[6] M. Fukada, M.K. Takimoto, K. Ogino and S. Ohkubo, Phys. Rev. C **80**, 064613 (2009).
[7] K.P. Artemov, M.S. Golovkov, V.V. Pankratov and V.P. Rudakov, Phys. At. Nucl. **58**, 177 (1995).
[8] J. John, C.P. Robinson, J.P. Aldridge and R.H. Davis, Phys. Rev. **177**, 1755 (1969).
[9] D. Frekers, R. Santo and K. Langanke, Nucl. Phys. A **394**, 189 (1983).
[10] M. Kimura and H. Horiuchi, Nucl. Phys. A **767**, 58 (2006).
[11] K.P. Artemov, *et al.*, Sov. J. Nucl. Phys. **52**, 408 (1990).
[12] J.C. van den Berg, *Wavelets in Physics*, Cambridge University Press (2004).
[13] A. Shevchenko, *et al.*, Phys. Rev. Lett. **93**, 122501 (2004).
[14] Y. Kalmykov, *et al.*, Phys. Rev. Lett. **96**, 012502 (2006).
[15] T. Wakasa, *et al.*, Phys. Lett. B **653**, 173 (2007).
[16] J.F. Ziegler, J. Appl. Phys / Rev. Appl. Phys. **85**, 1249 (1999).
[17] A.M. Lane and R.G. Thomas, Rev. Mod. Phys. **30**, 257 (1958).
[18] S.R. Riedhauser, Phys. Rev. C **29**, 1961 (1984).
[19] N. Curtis and J. Walshe, Nucl. Instr. and Meth. in Phys. Res. A **797**, 44 (2015).
[20] J. Walshe, *et al.*, J. Phys. Conference Series **569**, 012052 (2014).
[21] M. Norrby, *Alpha-cluster structures in medium light nuclei*, PhD thesis, Abo Akademi University (2011).
[22] S. Bailey, *et al.*, Phys. Rev. C **90**, 024302 (2014).
[23] E.P. Wigner, SIAM Review **9**, 1 (1967).
[24] S. Bjørnholm and J.E. Lynn, Rev. Mod. Phys. **52**, 725 (1980).
[25] R. Vandenbosch and J.R. Huizenga, *Nuclear Fission*, Academic Press (1973).
[26] T.A. Brody, *et al.*, Rev. Mod. Phys. **53**, 385 (1981).
[27] I.J. Thompson and F.M. Nunes, *Nuclear Reactions for Astrophysics*, Cambridge University Press (2009).